Received: 13 June 2023 | Revised: 19 November 2023 | Accepted: 19 December 2023

DOI: 10.1096/fj.202301069RR

RESEARCH ARTICLE

The FASEB Journal

Role of the CCL20/CCR6 axis in tubular epithelial cell injury: Kidney-specific translational insights from acute kidney injury to chronic kidney disease

Kyung Don Yoo[1,2] | Mi-yeon Yu[3] | Kyu Hong Kim[4] | Seongmin Lee[4] | EunHee Park[1] | Seongmin Kang[1] | Doo-Ho Lim[1] | Yeonhee Lee[5] | Jeongin Song[6] | Soie Kown[6] | Yong Chul Kim[6] | Dong Ki Kim[6] | Jong Soo Lee[1,2] | Yon Su Kim[6,7,8] | Seung Hee Yang[7,8]

[1]Department of Internal Medicine, University of Ulsan College of Medicine, Ulsan University Hospital, Ulsan, Republic of Korea

[2]Basic-Clinical Convergence Research Institute, University of Ulsan, Ulsan, Republic of Korea

[3]Department of Internal Medicine, Hanyang University Guri Hospital, Hanyang University, Seoul, Republic of Korea

[4]Department of Biomedical Sciences, Seoul National University College of Medicine, Seoul, Republic of Korea

[5]Department of Internal Medicine, Uijeongbu Euji Medical Center, Eulji University, Uijeongbu-si, Republic of Korea

[6]Department of Internal Medicine, Seoul National University College of Medicine, Seoul National University Hospital, Seoul, Republic of Korea

[7]Kidney Research Institute, Seoul National University, Seoul, Republic of Korea

[8]Biomedical Research Institute, Seoul National University Hospital, Seoul, Republic of Korea

Correspondence
Seung Hee Yang, Biomedical Research Institute, Seoul National University Hospital, 101 Daehakro Jongno-gu, Seoul 03080, Republic of Korea.
Email: ysh5794@gmail.com

Funding information
Ulsan University Hospital Research, Grant/Award Number: UUH-2020-08; National Research Foundation of Korea, Grant/Award Number: NRF-2022R1F1A107612912

Abstract

This study investigated the role of the axis involving chemokine receptor 6 (CCR6) and its ligand chemokine (C–C motif) ligand 20 (CCL20) in acute kidney disease (AKD) using an ischemia–reperfusion injury (IRI) model. The model was established by clamping the unilateral renal artery pedicle of C57BL/6 mice for 30 min, followed by evaluation of CCL20/CCR6 expression at 4 weeks post-IRI. In vitro studies were conducted to examine the effects of hypoxia and H_2O_2-induced oxidative stress on CCL20/CCR6 expression in kidney tissues of patients with AKD and chronic kidney disease (CKD). Tubular epithelial cell apoptosis was more severe in C57BL/6 mice than in CCL20 antibody-treated mice, and CCR6, NGAL mRNA, and IL-8 levels were higher under hypoxic conditions. CCL20 blockade ameliorated apoptotic damage in a dose-dependent manner under hypoxia

Abbreviations: AKD, acute kidney disease; AKI, acute kidney injury; ANOVA, one-way analysis of variance; BUN, blood urea nitrogen; CCL20, chemokine ligand 20; CCR6, chemokine receptor 6; CKD, chronic kidney disease; cTNFRs, circulating TNF receptors; EMT, epithelial-to-mesenchymal transition; FITC, fluorescein isothiocyanate; GFR, glomerular filtration rate; GN, glomerulonephritis; hTECs, primary human TECs; IgAN, immunoglobulin A nephropathy; IRI, ischemia-reperfusion injury; MIP-3 α, macrophage inflammatory protein-3 α; Nrf2, nuclear factor erythroid-derived 2-related factor; PBS, phosphate-buffered saline; PD, peritoneal dialysis; PF, peritoneal fibrosis; PI, propidium iodide; qRT-PCR, quantitative reverse transcription-PCR; RA, rheumatoid arthritis; ROS, reactive oxygen species; TECs, tubular epithelial cells; TGF-β, transforming growth factor-β.

Kyung Don Yoo and Mi-yeon Yu equally contributed to this study.

and reactive oxygen species injury. CCR6 expression in IRI mice indicated that the disease severity was similar to that in patients with the AKD phenotype. Morphometry of CCL20/CCR6 expression revealed a higher likelihood of $CCR6^+$ cell presence in CKD stage 3 patients than in stage 1–2 patients. Kidney tissues of patients with CKD frequently contained $CCL20^+$ cells, which were positively correlated with interstitial inflammation. CCL20/CCR6 levels were increased in fibrotic kidneys at 4 and 8 weeks after 5/6 nephrectomy. These findings suggest that modulating the CCL20/CCR6 pathway is a potential therapeutic strategy for managing the progression of AKD to CKD.

KEYWORDS

acute kidney injury, chemokine ligand 20, chemokine receptor 6, chronic kidney disease, hypoxia

1 | INTRODUCTION

Chemokines are a type of cytokine of approximately 8–10 kD that have the ability to stimulate leukocyte migration and directional movement (chemotaxis) via immune and inflammatory cascades.[1,2] The chemokine (C–C motif) ligand 20 (CCL20; i.e., macrophage inflammatory protein-3 α (MIP-3 α)) and its receptor chemokine receptor 6 (CCR6) play pivotal roles in inducing inflammatory reactions in various cells, including mucosal and skin cells, by activating epithelial cells and attracting Th17 cells to the site of inflammation.[3]

Chemokines were initially reported to act as a major mediator of inflammatory responses in animal models of rheumatoid arthritis (RA).[4] Since then, they have also been found in the synovial fluid,[4] lungs,[5] liver,[6] brain (during autoimmune encephalitis),[7] and other organs and have been shown to mediate disease development by controlling immune responses. CCL20 is a CC chemokine expressed in macrophages, dendritic cells, and lymphocytes, and CCR6 is a receptor of CCL20 expressed in Th17 cells, dendritic cells, and B cells. CCL20 acts on CCL6-expressing cells.[8] Th17 cells secrete CCL20 and express other CCL6s, which attract activated B, memory T, and immature dendritic cells and are involved in the migration of these cells in secondary lymphoid organs.[8,9] The CCL20/CCR6 axis is involved in synovial tissue destruction via the activation of fibroblast-like synoviocytes.[4] Compared with those in patients with osteoarthritis, CCL20 levels are increased in the synovial fluid and peripheral blood of patients with RA.[10,11] TNF-α, a key factor secreted from lymphocytes, causes inflammation and damages normal tissues. Infliximab, which recognizes and attaches to TNF-α, suppresses TNF action, thereby reducing the serum titer of CCL20 in patients with RA.[12] Inflammatory cytokine interactions with TNF-α, IL-1β, and IL-17 induce CCL20 expression, and cytokine-stimulated T lymphocytes can cause mononuclear mobilization with CCL20/CCR6 dependence.[9,13]

Research on the role of CCL20/CCR6 cascade in the context of kidney diseases is lacking. In an experimental glomerulonephritis (GN) model with autoimmune properties, CCR6 was found to be responsible for the reduction in the counts of both Tregs and Th17 cells; moreover, the reduction in the counts of anti-inflammatory Tregs resulted in the deterioration of renal function.[14] Similarly, this axis was revealed to be primarily involved in Th17 responses in another experimental GN model via transcriptomic analysis based on a Thy1.1 FSGS model[15,16] and an ANCA GN model.[15,16] In addition, kidney biopsy samples of patients with GN show increased expression of CCL20 in the sera and tissues of those with immunoglobulin A nephropathy (IgAN) via mesangial-infiltrating Th17 cells[17] as well as CCR6 expression[18]; however, the mechanisms underlying the Th17 pathway are poorly understood.

In this study, we propose that the CCL20/CCR6 pathway plays a pivotal role in the progression from acute kidney injury (AKI) to chronic kidney disease (CKD) by modulating immune and inflammatory responses. Currently, reliable diagnostic biomarkers to identify the transition from AKI to CKD are lacking. Therefore, we explored the role of CCL20/CCR6 as a regulatory factor in CKD progression, employing a comprehensive multiomics approach, including an examination of transcriptomic changes associated with the suppression of the CCL20/CCR6 axis during AKI.

2 | MATERIALS AND METHODS

All experiments were approved by the Institutional Animal Care and Use Committee in Seoul National

University Hospital (SNUH-IACUC), and animals were maintained in a facility accredited by AAALAC International (#001169) and treated in accordance with Guide for the Care and Use of Laboratory Animals 8th edition (NRC 2010, IACUC No: 20-0136-S1A0). All experiments dealing with human specimens were approved by the institutional review board at Seoul National University Hospital (IRB#: SNUH 2007-024-1139/UUH-2020-08).

The experimental methods used in the present study were based on previously described methods.[19–25] All experiments were conducted in accordance with the guidelines of the 2013 Declaration of Helsinki.

2.1 | Experimental animals for acute kidney injury and acute kidney disease

Male C57BL/6 (B6) mice (aged 8 weeks) were procured from the Orient Company (Seoul, Republic of Korea) and housed in a pathogen-free animal facility. Renal ischemia–reperfusion injury (IRI) was induced unilaterally and bilaterally following previously established experimental protocols.[19–24] Prior to the procedure, wild-type mice were anesthetized via an intraperitoneal injection using an anesthetic solution of tiletamine mixed with zolazepam (1:1) (Zoletil; 30 mg/kg of body weight; Virbac, USA) and xylazine (25 mg/mL) (Rompun; 10 mg/kg of body weight; Bayer, Canada).[25] Subsequently, bilateral flank incisions were performed, and both renal pedicles were carefully dissected and clamped using a microvascular clamp (Roboz Surgical Instrument, Gaithersburg, MD, USA) for 30 min.[19,20,23,26] Throughout the procedure, 2 mL of sterile saline at 40°C (1 mL during ischemia and 1 mL during reperfusion) was administered into the peritoneal cavity. Body temperatures were consistently monitored and maintained at 37°C during the renal IRI process. Following clamp removal, wounds were sutured, and adequate reperfusion was visually confirmed. Sham-operated mice underwent identical surgical procedures, with the exception of renal pedicle clamping. Mice were euthanized at 48 h post-reperfusion, and blood samples were collected from their tail veins. Unilateral IRI was also performed by clamping one renal vein and subjecting it to a 30 min ischemia–reperfusion period according to the protocol. The mice were sacrificed after a 4-week observation period following previously established experimental protocols. Finally, the anti-inflammatory effects in the mouse model of IRI were investigated by treating mice with a CCR6 antagonist (HY-151435, MedChemExpress, Monmouth Junction, NJ, USA),[27] both 1 h before the IRI procedure and again 12 h afterward.

2.2 | Experimental animals for chronic kidney disease

A rat model of CKD was developed using a modified protocol described in our previous study.[28] Male Sprague–Dawley rats weighing 160 to 200 g were purchased from the Jackson Laboratory. Upon arrival, the rats were allowed to acclimate to their new environment for approximately 1 week and provided ad libitum access to food and water. Prior to the surgery, an anesthetic solution of tiletamine mixed with zolazepam (1:1) (Zoletil; 30 mg/kg of body weight; Virbac) and xylazine (25 mg/mL) (Rompun; 10 mg/kg of body weight; Bayer) was administered via intraperitoneal injection. After confirming the anesthetized state of the rat, the surgical area was shaved and disinfected with an appropriate antiseptic solution. The rat was positioned on its back on a heating pad to maintain body temperature during the surgery. A small incision was made on the right flank to expose the right kidney; the kidney was carefully separated from the surrounding tissues; and the renal artery, renal vein, and ureter were isolated. The renal artery and vein supplying the upper and lower poles of the kidney were tied off with sutures. Then, approximately two-thirds of the kidney tissue were removed by resecting the upper and lower poles, taking care not to damage the renal pelvis or the ureter. After resection, the incision was closed with sutures, and an antibiotic ointment was applied. The rat was closely monitored during recovery and provided appropriate pain relief, such as buprenorphine (0.05 mg/kg), as necessary. After the rat resumed normal eating, drinking, and ambulatory activities, it was returned to its home cage. One week after the right kidney resection, the above process was repeated for left-side nephrectomy. The left nephrectomy marks the onset of moderate-to-severe renal failure in the rat. The rat's health status, including body weight, blood pressure, and urine output, were monitored. Additionally, blood and urine samples were collected periodically to assess renal function by measuring serum creatinine, blood urea nitrogen (BUN), and proteinuria.[28]

2.3 | Hypoxic cell culture conditions and primary culture of human tubular epithelial cells

The methods for establishing primary proximal tubule cell cultures have been described previously.[21,22,29,30] In brief, the kidney cortex was carefully sectioned, and the tissue pieces were treated with Hank's balanced salt solution containing 3 mg/mL collagenase (Sigma-Aldrich, St. Louis, MO, USA) and incubated at 37°C for 1 h. Next, the cells were rinsed with phosphate-buffered

saline (PBS) through a series of sieves and then spun down at 500×*g* for 5 min. Following this, the cells were treated with DMEM/F12 media (Lonza) for 4–6 h, after which the tubular cells floating in the media were harvested and grown on collagen-coated plates (BD Biosciences) until colonies of epithelial cells formed. Lastly, the tubular epithelial cells (TECs) were identified using a BD Biosciences fluorescence-activated cell sorting Calibur instrument with fluorescein isothiocyanate (FITC)-labeled anti-AQP1 stain (99.2%; Abcam, Cambridge, UK), applied at 4°C for 30 min (Figure S1), with podocalxylin-negative cells.

With the injury of primary cultured human TECs by the CCL20/CCR6 axis, in vitro tests were performed to reveal the function of CCL20/CCR6 inhibition in a hypoxic environment. The levels of IL-8, CCR6, and NGAL mRNA in primary TECs were examined under normoxic conditions. Cells were treated with either vehicle or anti-CCL20 antibody for 1 h and incubated in the presence of 1% oxygen (INCO 108 Incubator, Memmert, Schwabach, Germany) for 6 h to mimic AKI. Simultaneously, primary TECs were cultured in the presence of a monoclonal anti-CCL20 antibody at concentrations of 0, 1, and 2 μg/mL (#MA543911, Invitrogen, Thermo Fisher Scientific, Waltham, MA, USA), under hypoxic conditions (21% O_2, 5% CO_2, and 74% N_2), and reoxygenated after 6 h. Cells were extracted to assess the expression of CCR6 and NGAL to reflect an acute response to hypoxia and reoxygenation (21% O_2).[25,31] The concentrations of cytokines, including IL-8, were measured using a Bio-Plex Pro system (Bio-Rad Laboratories, Hercules, CA, USA).

2.4 | Real-time quantitative PCR analysis

Quantitative reverse transcription-PCR (qRT-PCR) analysis was conducted by extracting total RNA from renal tissues and cells following ischemia induction and then assessing cytokine mRNA concentrations using qRT-PCR. In brief, total RNA was isolated from kidney samples using a RNeasy kit (Qiagen GmbH, Hilden, Germany), and 1 μg total RNA was reverse-transcribed utilizing oligo-d(T) primers and AMV-RT Taq polymerase (catalog number A3500; Promega, Madison, WI, USA). qRT-PCR was conducted using the universal SYBR Green qPCR protocol (as detailed in the Supplementary Material; Table S1).

2.5 | Western blotting

Primary human TECs (hTECs) were processed in RIPA buffer containing a mixture of chemical agents (150 mM NaCl; 100 mM Na_3VO_4; 50 mM Tris–HCl, pH 7.3; 0.1 mM EDTA; 1% (vol/vol) sodium deoxycholate; 1% (vol/vol) Triton X-100; and 0.2% NaF) with protease inhibitor (GeneDEPOT, Texas, USA). The protein content of the cell lysate was measured using the BCA method. The proteins were separated by performing sodium dodecyl sulfate-polyacrylamide gel electrophoresis and were then transferred onto a polyvinylidene difluoride membrane (Millipore, Bedford, MA, USA). The membranes were blocked with a blocking agent (5% skimmed milk and 2% bovine serum albumin buffer) for 1 h and then treated with primary antibodies targeting ICAM-1 (Ab171123, Abcam), KIM-1 (MAA785Hu22, CLOUD-CLONE CORP, Houston, TX, USA), CCR6 (MBS2522958, MyBioSource, San Diego, CA, USA), and β-actin (A1978, Sigma-Aldrich). Next, protein–antibody complexes were detected using horseradish peroxidase-conjugated anti-rabbit IgG (7074S) and anti-mouse IgG (7076s, Cell Signaling Technology, Danvers, MA, USA). Proteins were visualized using Image Quant Las 4000 mini (Amersham plc, Amersham, UK) under optimal exposure time. Western blots were then semi-quantitatively analyzed using ImageJ (ImageJ Ver. 1.52a, Wayne Rasband, National Institutes of Health, USA) (Figure S1).

2.6 | Flow cytometry analysis (FACS) and annexin V/propidium iodide staining

For quantitative flow cytometry analysis, primary cultured human TECs cultured under oxidative stress were treated with a CCL20 antibody, and the isotype-positive TEC populations were detected. Flow cytometry was used to measure apoptosis and necrosis using Annexin V/propidium iodide (PI) FITC apoptosis reagent (BD Biosciences) according to the manufacturer's and previously described protocols.[24,32] In brief, 5×10^5 harvested cells were rinsed with cold PBS, suspended in 100 μL binding buffer, stained with 5 μL FITC-conjugated Annexin V (10 mg/dL) and 10 μL PI (50 mg/mL), and then incubated in the dark for 30 min at room temperature. Data were collected and analyzed using BD FACSDiva *v*.8.0 (BD Biosciences).

2.7 | Immunohistochemistry

Tissue samples were fixed with 10% buffered formalin and embedded in paraffin. Tissue sections (4 μm thick) were cut from paraffin blocks and subjected to dehydration and rehydration (in a series of xylene and decreasing concentrations of ethanol, followed by water). This was followed by overnight incubation in the presence of primary antibodies at 4°C. Unbound primary antibodies were

removed using several washes with PBS. Subsequently, cells were incubated with a secondary antibody for 1–2 h at room temperature. Unbound secondary antibody was removed following several washes of PBS, and slides were processed. The slides were then subjected to periodic acid-Schiff reagent staining and examined using an Olympus inverted microscope (Olympus Imaging America, Center Valley, CA, USA).[20]

The number of necrotic tubules and tubular casts relative to the total number of tubules was determined as described previously.[33] The degree of tubular injury was assessed by a renal histologist blinded to group assignment. Several key aspects were considered. First, we determined inflammatory cell infiltration, which refers to the influx of immune cells into the kidney tissue and is a hallmark of inflammation. In mild cases, only a few inflammatory cells are present in the tissue; in moderate cases, a noticeable increase in the number of inflammatory cells is observed, but they do not dominate the tissue; however, in severe cases, large numbers of inflammatory cells are present, potentially obscuring the normal tissue architecture. Second, we determined tubular atrophy, which refers to the shrinkage of tubular cells, leading to a reduction in their function. In mild cases, a small proportion of tubules show signs of atrophy; in moderate cases, a significant number of tubules are affected, but healthy tubules are still present; however, in severe cases, most tubules show signs of atrophy, indicating extensive damage. Third, we determined tubule fibrosis, which refers to the replacement of normal kidney tissues with fibrous connective tissue, leading to impaired kidney function. In mild cases, small areas of fibrosis are present, with minimal impact on overall kidney function; in moderate cases, a substantial amount of fibrosis is present, likely affecting kidney function; however, in severe cases, extensive fibrosis is present, with a significant impact on kidney function and structure. Finally, the extent of global sclerosis was evaluated and determined in terms of percentages.

2.8 | Immunofluorescence analysis and confocal microscopy

Immunofluorescence analysis was conducted using an LSM 510 META laser confocal microscope (Carl Zeiss, Jena, Germany). Paraffin-embedded samples were sectioned into 4-μm-thick slices. These samples were then deparaffinized and rehydrated using xylene and a graded series of ethanol solutions. The samples were then incubated with the primary antibodies specific for human CCR6 and CCL20 (Abcam) in a blocking reagent overnight at 4°C, followed by incubation with the secondary antibodies Alexa Fluor 488-conjugated goat anti-rabbit antibody (Molecular Probes, Eugene, OR, USA), Alexa Fluor 555-conjugated anti-rat antibody, and Alexa Fluor 555-conjugated anti-mouse antibody. All sections were washed and counterstained with 4′,6-diamidino-2-phenylindole for 5 min. Primary antibodies were omitted from the negative control.

2.9 | Human clinical sample study

The protocols for analyzing renal biopsy samples from patients with acute tubular necrosis (ATN) ($n = 13$) and normal controls ($n = 7$) were approved by the Institutional Review Board of Seoul National University Hospital (Table 1). The normal controls exhibited insignificant alterations in the glomeruli or tubules. Normal control group kidney tissues were sourced from renal biopsy samples of patients who showed no structural modifications. Slides were prepared using specimens from 56 patients who were clinically diagnosed with proteinuric CKD, with underlying etiologies of IgAN ($n = 55$) and diabetes mellitus nephropathy ($n = 1$; Table 2). The number of CCL20/CCR6 cells was determined using immunohistochemistry and morphometric analyses. The number of cells expressing CCL20 was determined using immunohistochemical staining and morphometric analyses. The count was tallied in five arbitrarily chosen fields from the biopsy tissue. Each kidney sample was examined under a light microscope at 100× magnification, and the percentage of the area showing CCL20 positivity was assessed using a morphometric system (Qwin 3, Leica, the Netherlands).

In this study, doubling of creatinine levels, an estimated glomerular filtration rate (GFR) reduction of 50%, and incident end-stage kidney disease requiring dialysis were defined as "CKD progression" for calculating kidney survival. Finally, serum CCL20 levels were analyzed, and clinical differences between CKD groups and the relation of CCL20 with circulating TNF receptors (cTNFRs) were investigated.[34]

2.10 | Statistical analyses

IBM SPSS Statistics *v*.21.0 (IBM Corporation, Armonk, NY, USA) and Prism *v*.8.4.1 (GraphPad Software, La Jolla, CA, USA) were used for data analysis. Kruskal–Wallis nonparametric testing was performed for multiple comparisons, and Mann–Whitney U testing, one-way analysis of variance (ANOVA) followed by Tukey's post-hoc analysis, and two-way ANOVA followed by Bonferroni post-hoc analysis were used to statistically analyze the data. Results with $p < .05$ were considered significant.

TABLE 1 Primary attributes of patients with acute tubular necrosis evaluated for CCL20 levels.

Case	Sex/Age[a]	Primary results of Bx	CCL20 (%)[b]	GS (%) on Bx finding	Serum Cr	eGFR	Alb	Hb	Urine PCR (g/g)	Tubular atrophy	Tubule fibrosis	Tubulitis
1	M/80	Ig MN	5.50	5.00	3.99	10	2.6	9.6	16.79	1	0	1
2	F/76	ATIN	8.91	0.00	4.3	10	1.9	9	30.83	2	0	2
3	F/59	IgAN	7.75	6.35	2.5	19.7	3.8	9.3	2.42	1	0	1
4	M/68	IgAN	5.92	15.00	2.06	32.2	3.9	9.3	0.58	1	0	1
5	F/49	ATN	11.94	3.30	1.7	31.9	3.7	11.7	0.15	1	0	1
6	F/31	ATIN	3.76	33.30	8.84	5.4	3	10.1	2.73	1	0	4
7	F/54	ATIN	7.07	23.10	1.8	31.5	4.1	7.6	2.04	2	0	4
8	F/29	ATIN	13.26	6.10	4.11	13.8	4.1	11.5	0.3	2	0	1
9	F/72	ATIN	9.73	28.60	2.48	19.1	3.1	9.8	1.74	3	0	3
10	F/74	ATIN	6.62	50.00	7.75	4.7	2.9	10.2	0.5	0	0	4
11	F/54	ATIN	4.18	23.10	1.87	30	4.1	8	2.04	2	0	4
12	M/60	ATIN	27.28	0.00	3.53	17.7	3.1	8.2	0.43	1	0	3
13	F/70	ATIN	7.21	21.10	5.62	7.1	3.9	9.2	0.5	1	0	4
1	F/21	NS	4.76	0.00	0.61	130	4.4	11.7	0.76	0	0	0
2	M/71	NS	3.61	0.00	1.17	54.8	3.9	16.8	0.19	1	0	0
3	M/53	NS	0.09	0.00	0.77	103.6	3.9	14.5	0.78	0	0	0
4	F/37	NS	0.05	2.00	0.78	97.4	3.8	10.5	0.1	0	0	0
5	F/63	NS	1.69	0.00	0.64	95.3	3.6	11.7	0.63	1	0	1
6	F/46	NS	1.81	0.00	0.67	94.5	4.4	11	0.01	0	0	0
7	F/51	NS	2.54	0.00	0.69	89.4	4.1	10.4	0.01	0	0	0

Note: Continuous variables are represented as the mean ± SD, and categorical variables are shown as frequency (%). Description of the kidney biopsy finding for tubule damage; absent 0, mild 1, moderate 2, marked 3, diffuse 4; Tubulitis, tubule with inflammatory cell infiltration.

Abbreviations: ATIN, acute tubulointerstitial nephritis; ATN, acute tubular necrosis; Bx, biopsy of kidney; Cr, Creatinine; eGFR, estimated glomerular filtration rate; GS, global sclerosis; Hb, hemoglobin; IgAN, immunoglobulin A nephropathy; Ig MN, immunoglobulin M nephropathy; NS, non-specific change; UPCR, urine protein-creatinine ratio.

[a]Age and laboratory data were provided at the time of Bx.

[b]CCL20 expression was measured by morphometric analysis of immunohistochemical (IHC) staining of kidney tissue.

TABLE 2 Baseline characteristics of patients with CKD subjected to CCR6 and CCL20 immunohistochemical (IHC) staining of kidney tissue.

N = 56	CKD stage 1/2 (*n* = 22)	CKD stage 3 (*n* = 18)	CKD stage 4/5 (*n* = 16)	*p* value
Age	34.27 ± 14.36	46.44 ± 10.83	47.00 ± 12.50	.003
Sex (male)	16 (72.6%)	11 (61.1%)	9 (56.2%)	.546
BMI	23.13 ± 3.24	24.05 ± 4.29	25.06 ± 2.90	.259
MDRD eGFR ($mL\,min^{-1}\,1.73\,m^{-2}$)	95.77 ± 26.34	46.27 ± 8.34	22.56 ± 6.43	<.001
Urine PCR ($mg\,g^{-1}$)	0.18 ± 0.66	1.56 ± 1.65	2.44 ± 2.78	.001
Proportion of nephrotic range PU (%)	1 (4.5%)	3 (16.7%)	3 (18.8%)	–
Hb ($g\,dL^{-1}$)	13.77 ± 1.54	12.05 ± 1.79	11.62 ± 1.99	.001
Albumin ($mg{\cdot}dL^{-1}$)	4.09 ± 0.42	3.77 ± 0.42	3.75 ± 0.44	.028
Kidney biopsy findings				
Inflammatory cell infiltration_moderate (%)	1 (4.5%)	8 (44.4%)	10 (62.5%)	.001
Tubular atrophy_moderate (%)	0 (0%)	6 (33.3%)	13 (81.2%)	<.001
Tubule fibrosis_moderate (%)	0 (0%)	6 (33.3%)	7 (43.8%)	<.001
Global sclerosis_percent_mean (%)	9%	34%	54%	<.001
CCR6 expression (%)	5.79 ± 5.97	10.94 ± 5.14	12.93 ± 5.51	.001
CCL20 expression (%)	2.92 ± 2.70	13.32 ± 5.65	10.18 ± 4.39	<.001

Note: Age and laboratory data were supplied at the time of biopsy. Continuous variables are expressed as means ± SD, while categorical variables are presented as frequency (%).

Abbreviations: BMI, body mass index; CKD, chronic kidney disease; Cr, creatinine; eGFR, estimated glomerular filtration rate; GS, global sclerosis; Hb, hemoglobin; NS, non-specific alteration; UPCR, urine protein-creatinine ratio.

3 | RESULTS

3.1 | CCR6 expression increased in renal tissues from patients with AKI

CCR6 expression levels in kidney tissues obtained from patients with ATN and normal kidney controls were compared. CCL20 expression was elevated in individuals with ATN. Table 1 shows the fundamental attributes of patients with ATN, as determined through immunohistochemistry. CCL20 expression was elevated in the tubulointerstitial area of human ATN tissues (Figure 1A). Additionally, the number of TECs showing elevated CCL20 expression was significantly larger in human ATN tissues than in the control group. In patients with ATN, a higher count of CCL20-positive cells in the kidney tissues correlated with increased levels of creatinine in the serum (Table 1). Kidney ischemia was induced in wild-type mice to identify the precise function of CCR6 in bilateral IRI in the kidneys; our results revealed that renal function deteriorated substantially following bilateral IRI (sham control vs. wild-type disease control Cr levels = 0.20 ± 0.02 mg/dL vs. 1.51 ± 0.11 mg/dL; $p < .001$, Figure 1B). The mRNA levels of inflammatory cytokines were re-evaluated using qRT-PCR, and the results revealed notable upregulation of NGAL, MCP-1, and CCL20 expression in wild-type mice compared with that in the sham controls ($p < .001$; Figure 1B). We further analyzed the role of CCR6 and its ligand CCL20 using in vitro and in vivo AKI models and determined the RNA levels of inflammatory cytokines. The results revealed notable upregulation of NGAL, MCP-1, and CCL20 expression in wild-type mice compared with that in the sham controls.

3.2 | CCR6 expression increased with cellular stress in primary cultured human TECs

The in vitro AKI model was used to determine whether oxidative stress increased CCR6 expression in primary hTECs. Blocking CCL20 reduced the levels of intracellular ICAM-1, reactive oxygen species (ROS), and 8-OHDG in hTECs subjected to oxidative stress (Figure 2A–C). ICAM-1, a cell adhesion molecule, was more strongly expressed under oxidative stress, and its expression reduced following CCL20 blockade; similarly, elevated levels of the oxidative stress markers ROS and 8-OHDG mRNA decreased in a dose-dependent manner. CCR6, NGAL mRNA, and IL-8 protein levels significantly increased under oxidative stress (Figure 2D). Furthermore, the levels of NGAL and IL-8 were significantly attenuated after administering the CCL20 blocking antibody in acute cell injury conditions, suggesting that CCR6 and CCL20 play a crucial

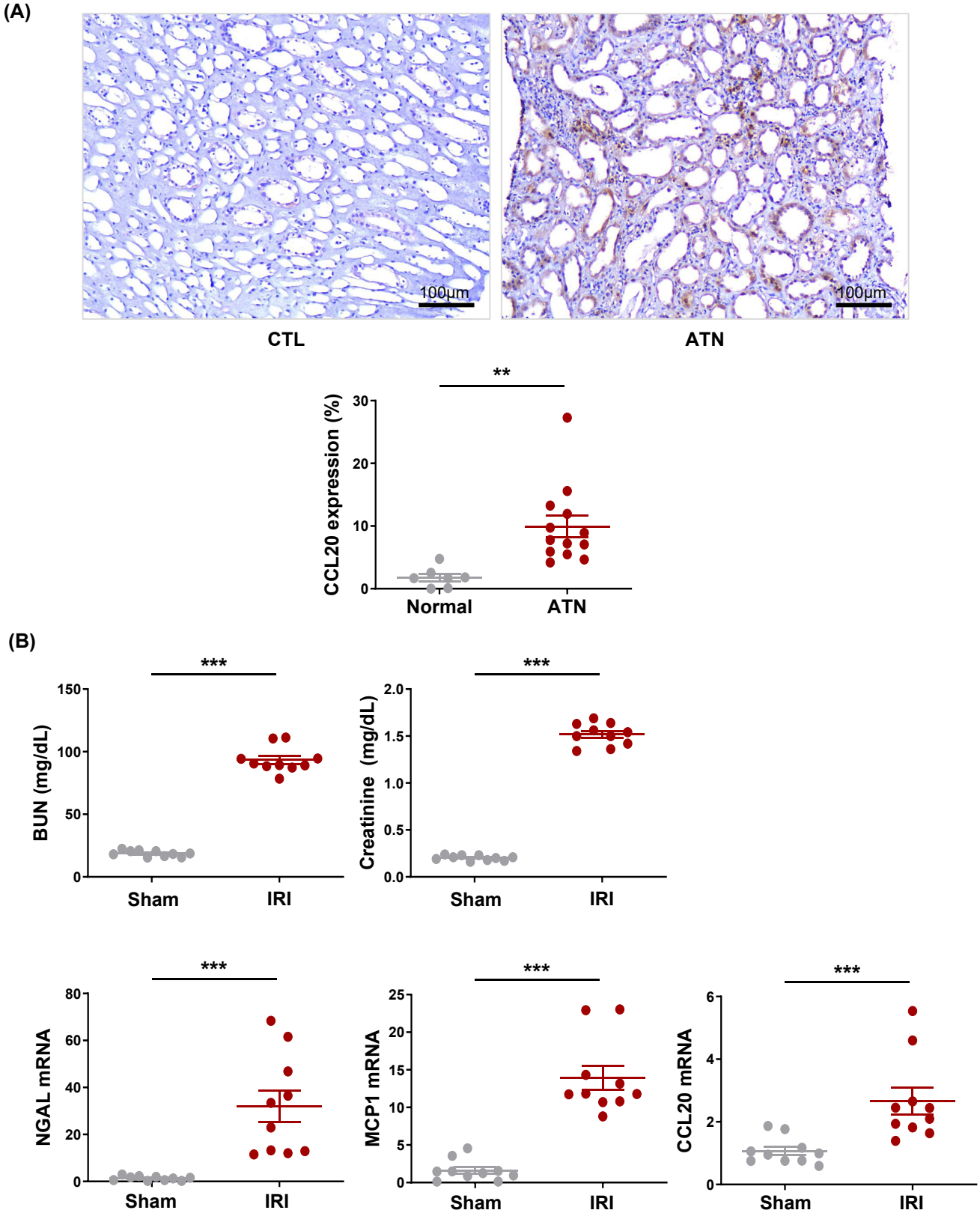

FIGURE 1 Increased CCL20 expression in AKI. Representative periodic acid-Schiff staining demonstrated enhanced uptake of CCL2 in kidney tissue of patients with ATN (A, Original magnification ×100). Bilateral ischemia–reperfusion injury in wild-type mice induced elevated mRNA levels of the inflammatory cytokines NGAL, MCP-1, and CCL20, as determined by real-time PCR analysis (B, $p < .001$). Sample size, $n = 10$ per group; *$p < .05$, **$p < .01$, ***$p < .001$. ATN, acute tubular necrosis; CTL, control; IRI, ischemia–reperfusion injury.

role in inducing AKI via oxidative stress and hypoxia. Consistently, the expression of the inflammatory marker ICAM-1 and kidney injury markers KIM-1 and CCR6 was significantly restored in a dose-dependent manner by blocking CCL20 (Figure 2E).

To induce hypoxic stress in hTECs, cells were initially cultured under 21% oxygen (normoxia), followed by 6 h culture in the presence of 1% oxygen (hypoxia), and then again 12 h culture in the presence of 21% oxygen (reoxygenation) as shown in Figure 2F. The CCR6 mRNA expression level significantly increased in response to hypoxia but decreased upon reoxygenation ($p < .001$). Conversely, the mRNA expression level of nuclear factor erythroid-derived 2-related factor (Nrf2), a transcription factor that activates various mechanisms in response to oxidative stress, decreased under hypoxia and exceeded normoxia levels before hypoxia.

3.3 | Apoptotic damage induced by acute cell injury was alleviated by CCL20 blocking

The number of apoptotic cells increased following oxidative (Figure 3A) and hypoxic (Figure 3B) stresses. Furthermore, the number of apoptotic cells was significantly reduced after CCL20 blocking antibody treatment, with the two being negatively correlated with CCL20 blocking antibody dosage. Flow cytometry images were used to identify the anti-apoptotic population of TECs treated with H_2O_2. Expression of Annexin$^+$/PI$^+$ in TECs was elevated as a result of oxidative stress, with the following percentages of the Annexin$^+$/PI$^+$ cell population observed in each condition: 3.12 ± 0.24% when the reference was used, 17.46 ± 0.85% with H_2O_2, 10.36 ± 0.90% with 1 μM anti-CCL20 antibody, and 7.33 ± 1.42% with 2 μM anti-CCL20 antibody. FACS pictures of the Annexin/PI labeling analysis were also used to identify the anti-apoptotic population of TECs exposed to hypoxia. TECs exhibited increased Annexin$^+$/PI$^+$ expression levels following hypoxia. The following percentages of the Annexin$^+$/PI$^+$ cell population were observed under each condition: 3.47 ± 0.46% in normoxia, 13.90 ± 1.60% following 6 h hypoxia, 10.43 ± 1.07% with 1 μM anti-CCL20 antibody, and 6.56 ± 1.20% with 2 μM anti-CCL20 antibody.

3.4 | CCL20/CCR6 axis expression increased in patients with CKD

Next, we assessed the levels of CCL20/CCR6 expression in both the kidney tissue and serum samples collected from individuals diagnosed with CKD, differentiating the analyses according to CKD grade. Pertinent baseline characteristics of patients with CKD who were included in the immunohistochemistry analysis are summarized in Table 2, while those of patients included in the enzyme-linked immunosorbent assay are listed in Table 3. As the CKD grade increased, proteinuria became more pronounced, GFR decreased, and the pathological findings revealed more severe tubular atrophy and fibrosis (Table 2). The expression of CCL20/CCR6 increased in tubulointerstitial areas of human CKD tissues (Figure 4A). Notably, CCL20/CCR6 expression positively correlated with the stage of CKD (Figure 4B). In addition, a positive correlation was observed between CCL20 and CCR6 expression in kidney tissue of patients with CKD ($r = .6341$, $p < .0001$; Figure 4C). Histologically, as tubular atrophy and fibrosis increased, CCL20/CCR6 expression increased according to the advanced CKD grade (Figure 4D). These findings are consistent with apoptosis observed in the human TECs subjected to oxidative and hypoxia stresses (Figure 3). Based on the definition of "renal death" applied in this study (doubling of creatinine levels, estimated 50% GFR reduction, and start of renal replacement therapy), the high CCL20/CCR6 expression was not significantly related to renal survival ($p = .309$; Figure 4E). CCL20 levels increased as the CKD grade increased, but these changes were not significant (Table 3).

3.5 | Expression of the CCL20/CCR6 axis increased from AKI to CKD in vivo

To investigate the role of the CCL20/CCR6 axis in the progression from AKI to CKD, a rat model of 5/6 nephrectomy (Figure 5) and a mouse model of unilateral IRI (Figure 6) were established. Sirius red staining demonstrated that unilateral 5/6 nephrectomy-induced fibrosis worsened from 4 to 8 weeks, with the CCL20/CCR6 axis being prominently involved, unlike in sham-operated controls (Figure 5A). Moreover, the development of azotemia, elevation of creatinine levels, and onset of hypertension provided clear evidence for the successful establishment of an AKI to CKD model (Figure 5A). Quantitative RT-PCR analysis of CCR6 mRNA demonstrated that the fibrotic injury caused by the 5/6 nephrectomy procedure affected the survival of tubular cells at both 4 and 8 weeks, as indicated by alterations in CCL20 and CCR6 levels. Notably, while the expression of the CCL20 mRNA significantly increased at 8 weeks compared with that at 4 weeks, no substantial changes were observed in CCR6 levels (Figure 5B).

To examine the role of CCL20/CCR6 in the progression from AKI to CKD, unilateral IRI was introduced in the kidneys of mice. Sirius red staining revealed that unilateral

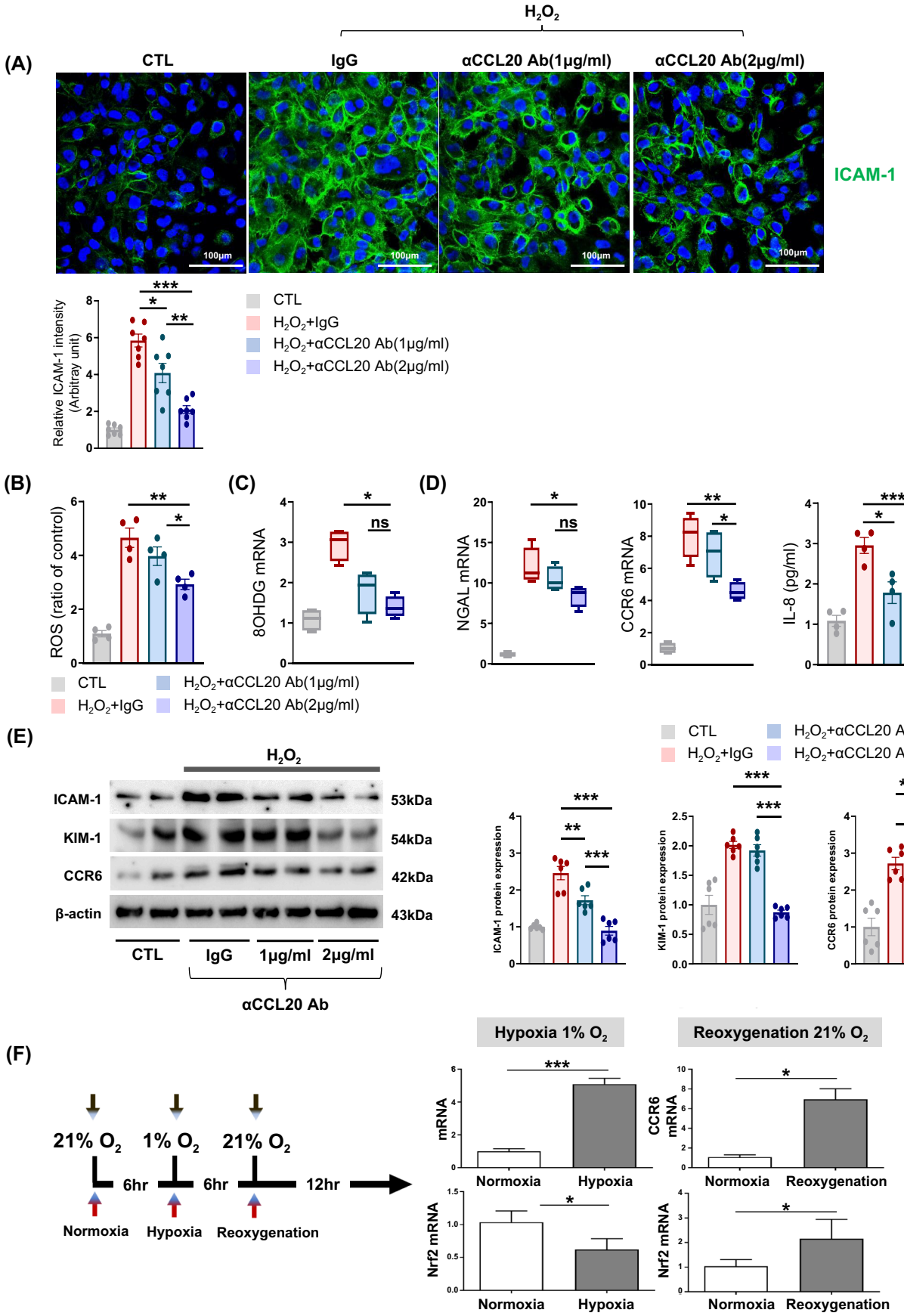

FIGURE 2 Effect of CCL20 blockade on an in vitro AKI model. The administration of CCL20 blocking antibody at doses of 1 and 2 μg/mL reduced ICAM-1 expression (A) and resulted in dose-dependent reductions in ROS levels (B), 8-OHDG mRNA (C), and mRNA levels of NGAL and CCR6, and IL-8 levels (D). Levels of ICAM-1, KIM-1, and CCR6, significantly decreased in a dose-dependent manner following CCL20 blockade (E). Assessment of CCR6 and Nrf2 mRNA levels during normoxia, hypoxia, and reoxygenation showed an increase in CCR6 expression but a decrease in the Nrf2 expression under hypoxic and reoxygenation conditions (F). Sample size, $n = 6$ per group; $^{*}p < .05$, $^{**}p < .01$, and $^{***}p < .001$.

IRI resulted in fibrosis, altered kidney size (Figure 6A) and was positively correlated with CCL20/CCR6 levels (Figure 6B).

3.6 | Modulation of the CCL20/CCR6 axis mitigates AKI progression in a mouse model of bilateral IRI

To elucidate the involvement of the CCL20/CCR6 axis in AKI progression, we employed a bilateral IRI mouse model (Figure 7A). A CCR6 antagonist (1 and 2 mg/kg) was subcutaneously administered at 1 h before and after inducing bilateral renal ischemic injury. Subsequently, we assessed AKI at 24 h post-injury by assessing serum markers and kidney tissues. Following bilateral IRI, a significant increase in BUN and creatinine levels was observed, which is indicative of AKI. Remarkably, the administration of the CCR6 antagonist significantly reduced the severity of azotemia (Figure 7B). Furthermore, CCR6 antagonist treatment effectively mitigated kidney damage. Specifically, levels of both F4/80 and NGAL reduced, highlighting the therapeutic potential of CCR6 antagonist administration in ameliorating renal injury in the bilateral IRI model (Figure 7C). Additionally, ICAM-1 and NGAL mRNA expression levels in serum were substantially increased post AKI. However, following CCR6 antagonist administration, the levels reduced significantly (Figure 7D). These findings suggest that treatment with CCR6 antagonists may attenuate AKI progression.

4 | DISCUSSION

To our knowledge, this study is the first to demonstrate the role of the CCL20/CCR6 axis in TEC injury during kidney IRI. Oxidative and hypoxic conditions increased mRNA expression of CCR6 and NGAL and IL-8 levels compared with normal conditions. However, CCL20 blockade reduced these levels and alleviated apoptotic damage in a dose-dependent manner in a primary culture of human TECs subjected to hypoxia and ROS injury. Moreover, CCL20 blockade significantly reduced intracellular ROS, 8-OHDG, and ICAM-1 levels. Analysis of CCL20/CCR6 expression from 22, 18, and 16 patients with CKD at stages 1–2, 3, and 4–5, respectively, showed that stage 3 patients were more likely to possess CCR6 cells in their kidneys than stage 1–2 patients. Furthermore, kidney tissues from patients with CKD frequently contained $CCL20^{+}CCR6^{+}$ cells, which positively correlated with interstitial inflammation according to CKD stage. The CCL20/CCR6 axis facilitated inflammatory cell (e.g., lymphocytes and macrophages) recruitment to the kidney injury site. These cells produced various inflammatory mediators, such as cytokines and growth factors, which further exacerbated tissue damage and promoted fibrosis development.

The main strength of the present study lies in the observation of CCL20/CCR6 expression in the tissues and serum of both CKD and AKI patients and the substantiation of these findings in animal and cellular models. Welsh-Bacic et al. found many CCR6-positive B and T cells in tubulointerstitial regions in patients with IgAN.[18] Furthermore, approximately half of the CD20-positive cells were also CCR6-positive, suggesting a role for CCR6 in the activation or recruitment of these cells in patients with IgAN. While CCR6 expression decreased in glomerular endothelial cells, CCR6 and CCL20 expression increased in the interstitial area, especially in IgAN.[18] The consistent results for CCR6 and tubulointerstitial inflammation scores suggest that as kidney disease progresses, the role of CCR6 may shift from glomeruli to tubulointerstitial in IRI. CCR6 was identified as a potential mediator of ARB effects in anti-Thy-1.1 GN,[16] which is consistent with observations in human patients with IgAN. The notable lack of glomerular CCR6 staining suggested that during telmisartan treatment, CCR6 may be primarily functional in tubulointerstitial regions. In a preliminary investigation using a rat model of 5/6 nephrectomy-induced kidney fibrosis for transcriptomics, RNA sequencing analysis of kidney tissues in this model revealed the significant upregulation of genes associated with CCL20 and CCR6 (data not shown). Our research also confirmed the correlation between CCR6/CCL20 expression and the renal damage degree; 56 patients with proteinuric CKD presented underlying etiologies of IgAN ($n = 55$) and diabetes mellitus nephropathy ($n = 1$), as confirmed through kidney biopsy. The CCR6/CCL20 chemokine profile was prominently altered in IgA1-treated human mesangial cells in Chinese patients with IgAN.[17] Specifically, serum CCL20 levels were significantly elevated in patients with

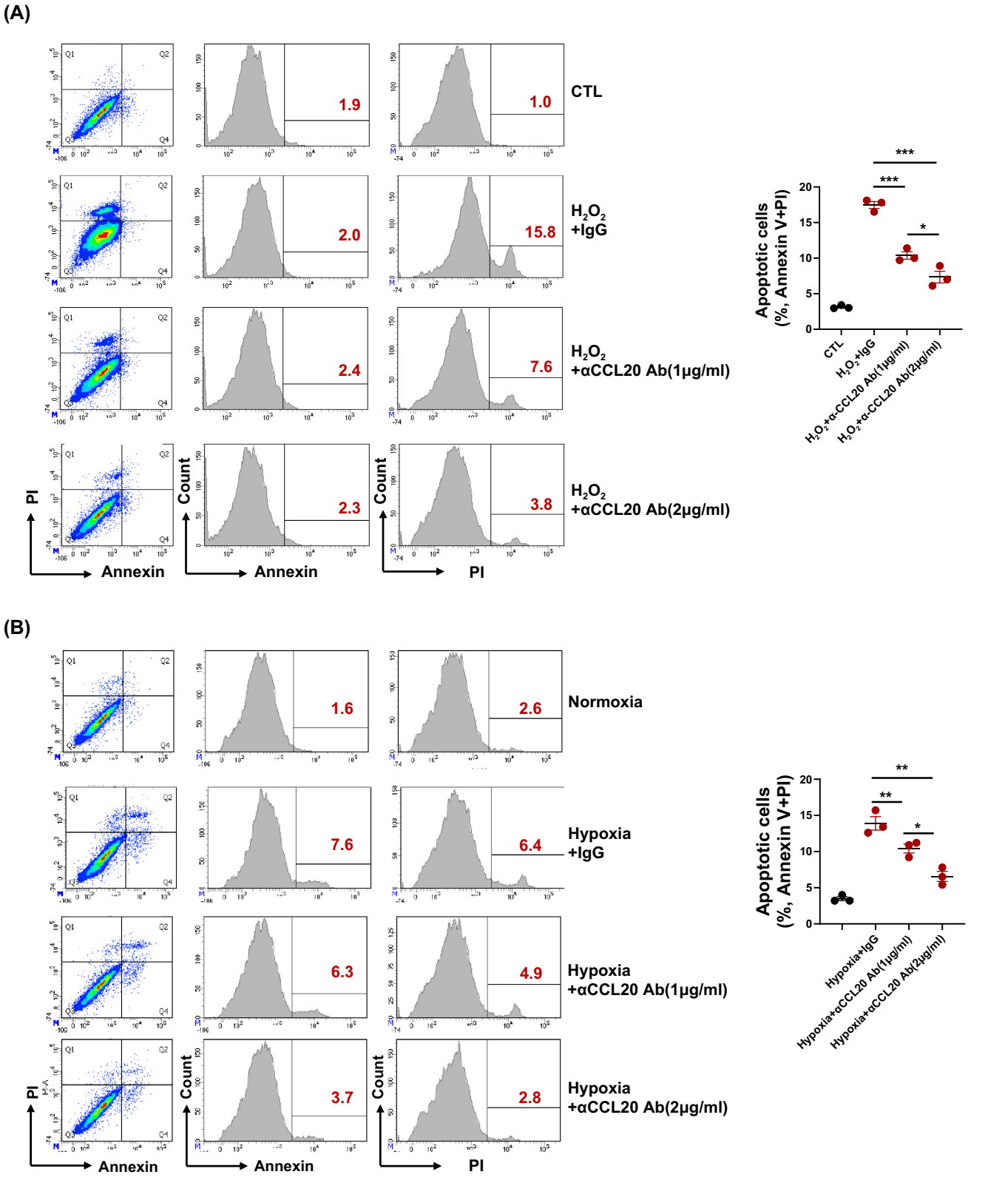

FIGURE 3 Annexin V/Propidium iodide staining assay. The number of apoptotic cells increased in oxidative stress (A) and hypoxic states (B) compared to those under the normoxic state. Treatment with CCL20 blocking antibody resulted in a decrease in apoptotic cells. The anti-apoptotic effect of the anti-CCL20 mAb was confirmed by Annexin V/propidium iodide staining using pPTCs ($n = 3$). The histogram on the right of the figure presents the percentage (sum) of Annexin V positive or PI positive cells in the dot plots. Sample size, $n = 3$ per group, $^{*}p < .05$, $^{**}p < .01$, and $^{***}p < .001$. PI, propidium iodide; pPTCs, primary proximal tubule cells.

TABLE 3 Baseline characteristics of patients with CKD analyzed for the serum CCL20 expression.

N = 55	CKD stage 1/2 (*n* = 11)	CKD stage 3 (*n* = 34)	CKD stage 4/5 (*n* = 10)	*p*-Value
Age	32.0 ± 7.9	51.8 ± 15.0	53.6 ± 15.5	<.001
Sex (male) (%)	5 (45.5)	21 (61.8)	7 (70.0)	.489
BMI	24.5 ± 3.5	24.8 ± 3.9	23.9 ± 3.4	.807
Serum Cr	0.7 ± 0.1	1.7 ± 0.5	3.3 ± 1.0	<.001
MDRD eGFR ($mL\,min^{-1}\cdot 1.73\,m^{-2}$)	105.1 ± 12.8	42.6 ± 9.4	21.4 ± 1.8	<.001
Cystatin C	0.6 ± 0.1	1.3 ± 0.3	2.4 ± 0.6	<.001
UPCR ($mg\,g^{-1}$)	0.2 ± 0.5	1.3 ± 2.0	3.8 ± 4.1	.007
Systolic blood pressure (mmHg)	116.6 ± 10.0	126.7 ± 16.2	130.0 ± 18.6	.114
Hb ($g\,dL^{-1}$)	14.1 ± 1.3	13.0 ± 1.7	10.9 ± 1.8	<.001
Albumin ($mg\,dL^{-1}$)	4.3 ± 0.3	4.1 ± 0.3	3.8 ± 0.4	.030
Total cholesterol	162.1 ± 25.5	179.5 ± 27.5	161.4 ± 25.0	.066
Uric acid	4.6 ± 1.5	6.7 ± 1.4	7.8 ± 1.3	<.001
TNFR1	886.2 ± 394.5	2217.0 ± 1006.5	3744.9 ± 1488.2	<.001
TNFR2	1832.7 ± 758.8	4437.1 ± 2028.0	7995.7 ± 3246.9	<.001
CCL20 expression ($pg\,mdL^{-1}$)	10.0 ± 8.4	21.29 ± 27.7	25.6 ± 29.9	.335

Note: Continuous variables are expressed as mean ± SD, while categorical variables are presented as frequency (%).

Abbreviations: BMI, body mass index; CKD, chronic kidney disease; Cr, creatinine; eGFR, estimated glomerular filtration rate; GS, global sclerosis; Hb, hemoglobin; NS, non-specific alteration; TNFR, tumor necrosis factor receptor; UPCR, urine protein-creatinine ratio.

IgAN and IgA1-treated human mesangial cells. CCR6 was highly expressed in activated T cells, and intracellular staining and cytokine expression profiles suggested that CCR6+ T cells produced high IL-17 levels.[17] Overall, our findings are in alignment with those of Lu et al. However, while we observed increased tissue expression of CCR6/CCL20, establishing a clear correlation with serum CCL20 titer proved challenging (Table 2). This disparity may be attributed to the high systemic and tissue chemokine levels; moreover, even if a difference is not observed in serum, the increased expression in tissues could be used as an early marker of IRI.

In AKI, the outer medullar proximal S3 segment TECs are the most sensitive to acute ischemic and nephrotoxic damage resulting from excessive metabolic load, high metabolic demand, and limited anaerobic energy production.[35] These areas also present a unique microvascular environment with high susceptibility to renal ischemia, renal hypoxia, and mitochondrial damage.[35,36] In TEC injury, inflammatory cytokines are generated (e.g., IL-6, IL-1 β, and TNF-α), which directly affect macrophage activation.[37,38] Macrophages are a major source of chemokine expression in AKI. Chemokine expression also affects macrophage migration[23] and subsequently upregulates reactive oxygen radicals and adhesion molecules.[39] Among the chemokines involved in TEC injury, CCL20 and its role were first elucidated by Ramos et al. using a model of folic acid-induced AKI,[40] and CCL20 blockade aggravated renal injury caused by high-dose folic acid. Turner et al. revealed that $FoxP3^{+}CD4^{+}$ and IL17-producing $CD4^{+}$ cells exhibited higher Treg counts and CCR6 expression, whereas IFN-r Th1 cells were CCR6-negative.[14] Furthermore, in a GN model, severe renal injury was further aggravated in CCR6 KO mice owing to the lack of convergence of Tregs and Th17 cells, whereas Th1 cells were unaffected. Consequently, injury was suppressed in CCR6 KO mice following the injection of Tregs obtained from wild-type mice, indicating the protective effect of CCR6. With respect to the CCL20/CCR6 pathway, Treg and Th17 cell regulation affected inflammation. In our study, we detected a notable increase in CCL20 expression during AKI, which is consistent with previous observations in patients with ATN and mouse models of bilateral IRI. Notably, our analysis highlighted distinct and prominent CCL20 staining in the TECs of patients with ATN, thereby corroborating the patterns documented in earlier investigations.

The results of both experimental studies were inconsistent with the main finding from the present study. In folic acid-induced TEC injury, CCL20 was found to play a protective role against kidney injury; moreover, when anti-CCL20 antibody was injected, $CCR6^{-/-}$ mice showed enhanced TEC injury.[40] Regarding these results, the influence of other cytokines and cell-surface cytokine receptors cannot be overlooked. Th17 cells express receptors CCR6 and CXCR3, and the Treg cells express receptors CCR4, 5, 6, and 8 and CXCR3 and CXCR6, implying a possible change in directionality caused by other cytokines. Ischemic AKI is associated with

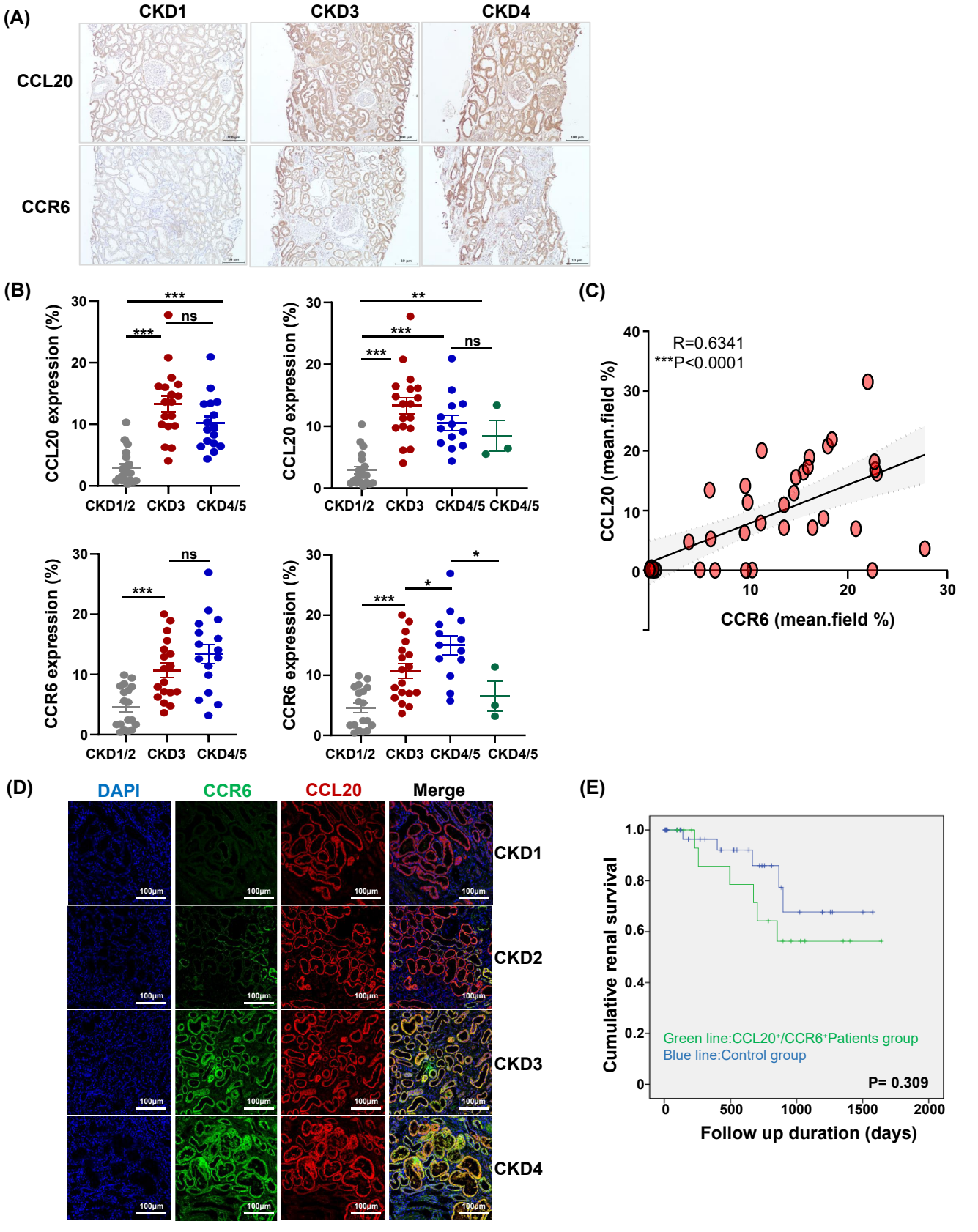

CXCR3, PD-1, CD44, ST2, and CD73 in Tregs.[13] Another study found that 60% Th17 cells were CCR6$^+$ but only 20% of Tregs were CCR6$^+$.[2] Additionally, in the presence of functional Th1 cells, Treg and Th17 cell recruitment is induced by CCR6, and GN is aggravated owing to the decline in the number of anti-inflammatory Tregs.[14]

FIGURE 4 Immunohistochemical insights into chronic kidney disease. Immunohistochemical staining of kidney tissue was performed to compare the expression of CCL20/CCR6 in tubular epithelial cells across different stages of chronic kidney disease (CKD) (A, original magnification ×400). The expression of CCL20/CCR6 increased with CKD severity quantified in kidney tissue (B). Immunofluorescence analysis confirmed a positive correlation between CCL20 and CCR6 expression in kidney tissue of patients with CKD (C). Confocal microscopy revealed that advanced stages of CKD exhibited increased tissue expression of CCL20+/CCR6+ (D, original magnification ×400). Evaluation of renal survival, based on a 50% reduction in estimated glomerular filtration rate or the initiation of kidney replacement therapy, indicated that patients with >50% expression of both $CCL20^{+}/CCR6^{+}$ had a tendency toward decreased renal survival compared to the control group (E).

Recovery or injury occurs depending on the more dominant response to each factor and should be determined based on interactions with other cytokines and $CD4^{+}$ cells. Moreover, different mechanisms may be responsible for folic acid-induced AKI and IRI AKI. Pathologic findings and mechanisms related to the cause of AKI were recently reported.[41] Changes in membrane architecture induced by oxidative stress were identified as the key mechanism underlying folic acid-induced AKI.[42] Although CCL20 levels increase in both folic acid-induced injury and unilateral ureteral obstruction (UUO) models, CCL20 blockade does not affect either in vitro or in vivo UUO models.[40] IRI involves Th17 because it is caused by ischemia and reperfusion.[22] However, the reported roles of Th17-CCL20 vary across different diseases. Therefore, the effects of Th17-CCL20 may vary according to the mechanism(s) underlying AKI. Moreover, a pleiotropic effect may have resulted from the time sequence differences in the CCL20/CCR6 axis injury.[9] In our study, CCL20 and CCR6 expression was investigated under various experimental conditions in hTECs, including 30 min for IRI; 30 min for hypoxia; 3, 6, and 24 h for reperfusion; 6 h for hypoxic damage and 24 h for hyperoxia. Additionally, detection was performed 2 d after folic acid injection using the folic acid assay and 5 d later using the UUO model.[40] CCR6 was expressed not only in Treg and Th17 cells but also in dendritic cells and macrophages. The plasticity of monocytes/macrophages transitioned to a reparative phenotype following 48 h of tubular injury, indicating a transition from an "inflammatory" to "pro-inflammatory" state.

Increased CCL20 expression occurs in the synovial fluid of patients with RA and is targeted by anti-rheumatic drugs.[12] Our study confirmed increased CCL20 levels in the blood of patients with CKD (Table 2). Notably, CCL20 expression was higher in patients with stage 3 CKD and slightly decreased in stage 4–5 patients. This pattern was also observed in the 5/6 rat nephrectomy model, where CCL20 mRNA expression increased earlier at 4 weeks post-disease induction. These findings suggest that CCL20 levels may initially increase during early kidney damage, leading to an interaction with CCR6, which promotes disease progression. Although the possibility of Th17-mediated autoimmune kidney disease is suggested, research regarding the role of the CCL20/CCR6 axis in the AKI-to-CKD transition is lacking (Table 4). Accordingly, further research is warranted, especially in relation to the role of Th17 pathway in ischemic AKD. According to a recent systematic review,[43] patients with damaged kidneys surpassing AKI may have historically been classified into a different disease group known as AKD.[44] Although the mechanism underlying AKI is not fully understood and how CCL20/CCR6 accelerates or causes progression of CKD is unknown,[44] our findings suggest that targeting the CCL20/CCR6 pathway may be a novel therapeutic approach for AKI-to-CKD transition.

Despite our promising results, our study has some limitations regarding thoroughly addressing the AKI-to-CKD transition. Our experimental design employed two distinct models representing AKI and CKD and thus lacks a direct link connecting the two phases, impeding our ability to unequivocally establish the role of the CCL20/CCR6 axis in mediating this transition. To effectively investigate and validate this transition, a single animal model should be established that accurately simulates the progression from acute to chronic kidney injury. This model can provide concrete evidence on whether the inhibition of the CCL20/CCR6 axis effectively curtails the progression from AKI to CKD. To gain a deeper understanding of disease progression, forthcoming studies should knockdown or downregulate the CCL20/CCR6 axis in animal models. These experiments hold the potential to provide invaluable insights into the precise role of the CCL20/CCR6 pathway in disease progression and its viability as a therapeutic target. Furthermore, exploring the involvement of the CCL20/CCR6 axis in glomerular cells, fibroblast cells, and other renal cell types is crucial. Understanding crosstalk mechanisms and their contributions to disease progression will provide comprehensive insights into therapeutic interventions for AKD-to-CKD transition. Therefore, future studies should encompass a broader range of cell types and investigate their interactions within the context of the CCL20/CCR6 pathway.

In conclusion, while our study contributes valuable insights into the potential of targeting the CCL20/CCR6 pathway for managing the transition from AKD to CKD,

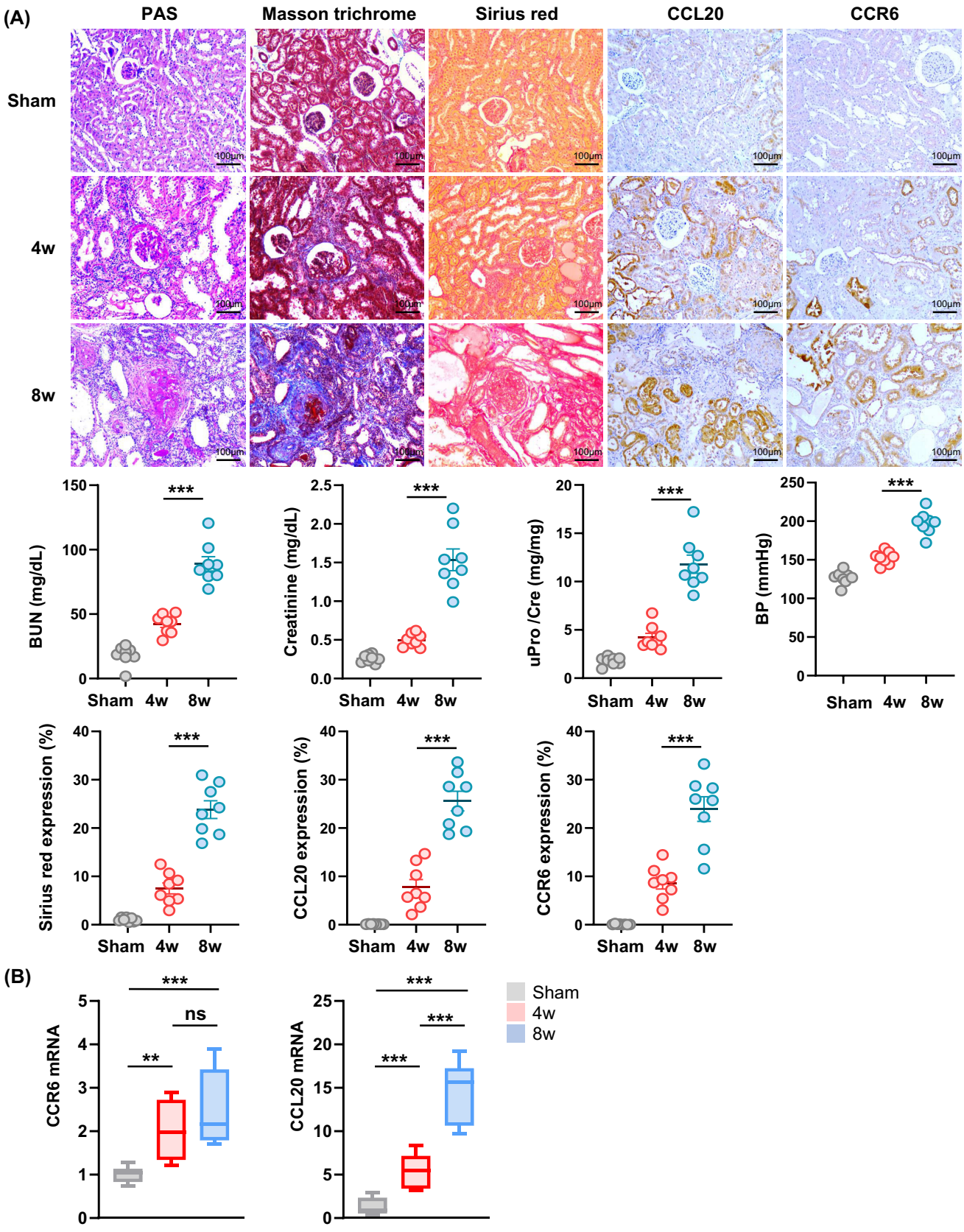

FIGURE 5 Expression of CCR6 and CCL20 in the Rat Model of 5/6 Nephrectomy. The rat model of 5/6 nephrectomy displayed increased CCL20/CCR6 expression in kidney tissue following 8 weeks of chronic injury, accompanied by the development of azotemia, proteinuria, and hypertension (A). The mRNA levels of CCL20/CCR6 increased following 5/6 nephrectomy in the presence of chronic kidney injury, with the severity of expression differences varying depending on the duration (B, $p < .001$). Sample size, $n = 8$ per group; $^{*}p < .05$, $^{**}p < .01$, and $^{***}p < .001$.

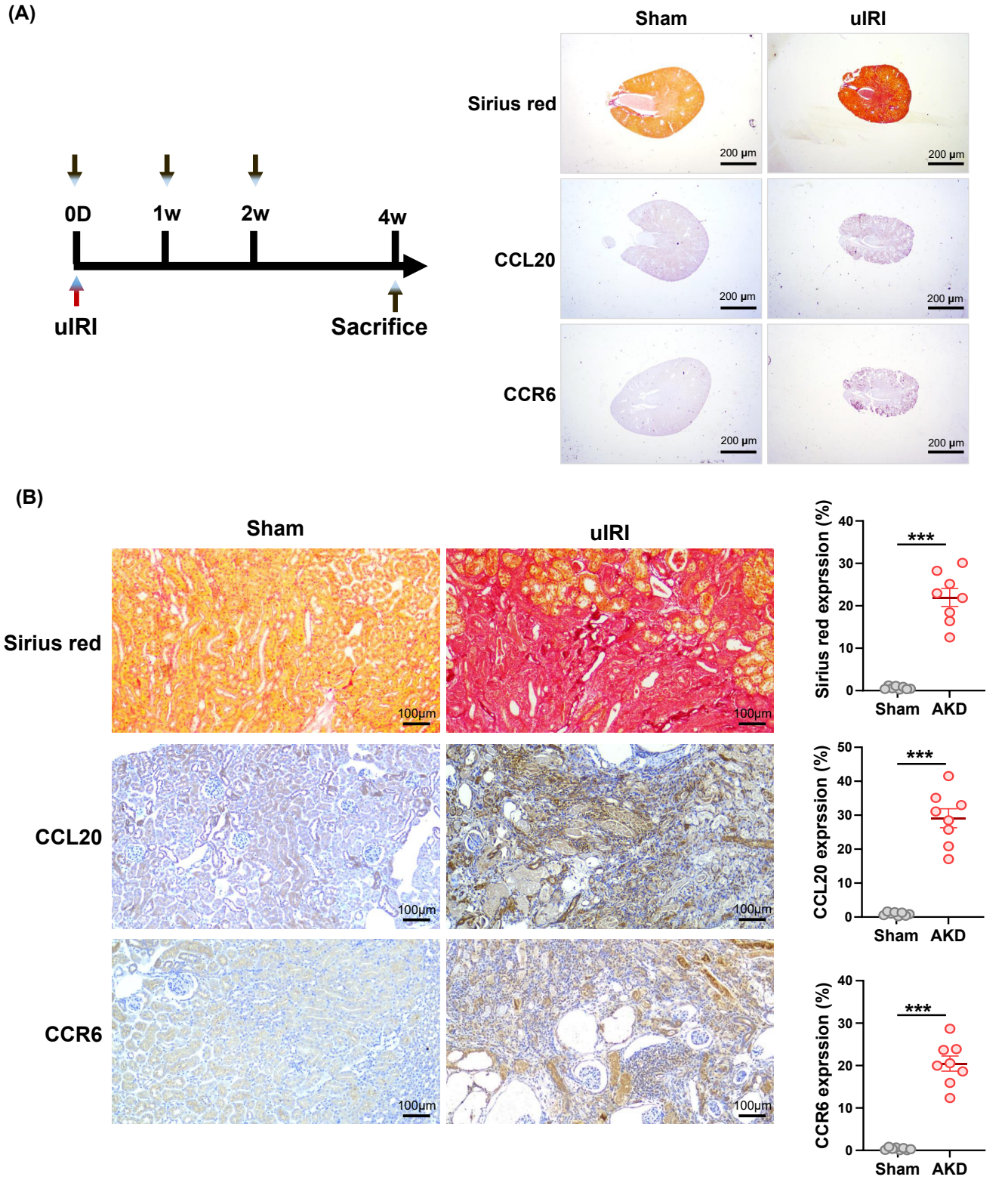

FIGURE 6 Expression of CCR6 and CCL20 in an acute kidney disease model induced by unilateral ischemia–reperfusion injury. Unilateral ischemia–reperfusion injury (uIRI) was induced in mouse kidneys to simulate acute kidney disease (AKD), resulting in minor kidney shrinkage. Sirius red staining of the damaged kidney tissue (A, original magnification ×200) revealed irreversible fibrotic changes. The kidneys affected by AKD exhibited expression of CCL20/CCR6 (A, B), and quantification of kidney tissue demonstrated a significant increase in CCL20 and CCR6 levels in the kidneys with unilateral IRI (B, $p < .001$, original magnification ×100). *$p < .05$, **$p < .01$, and ***$p < .001$.

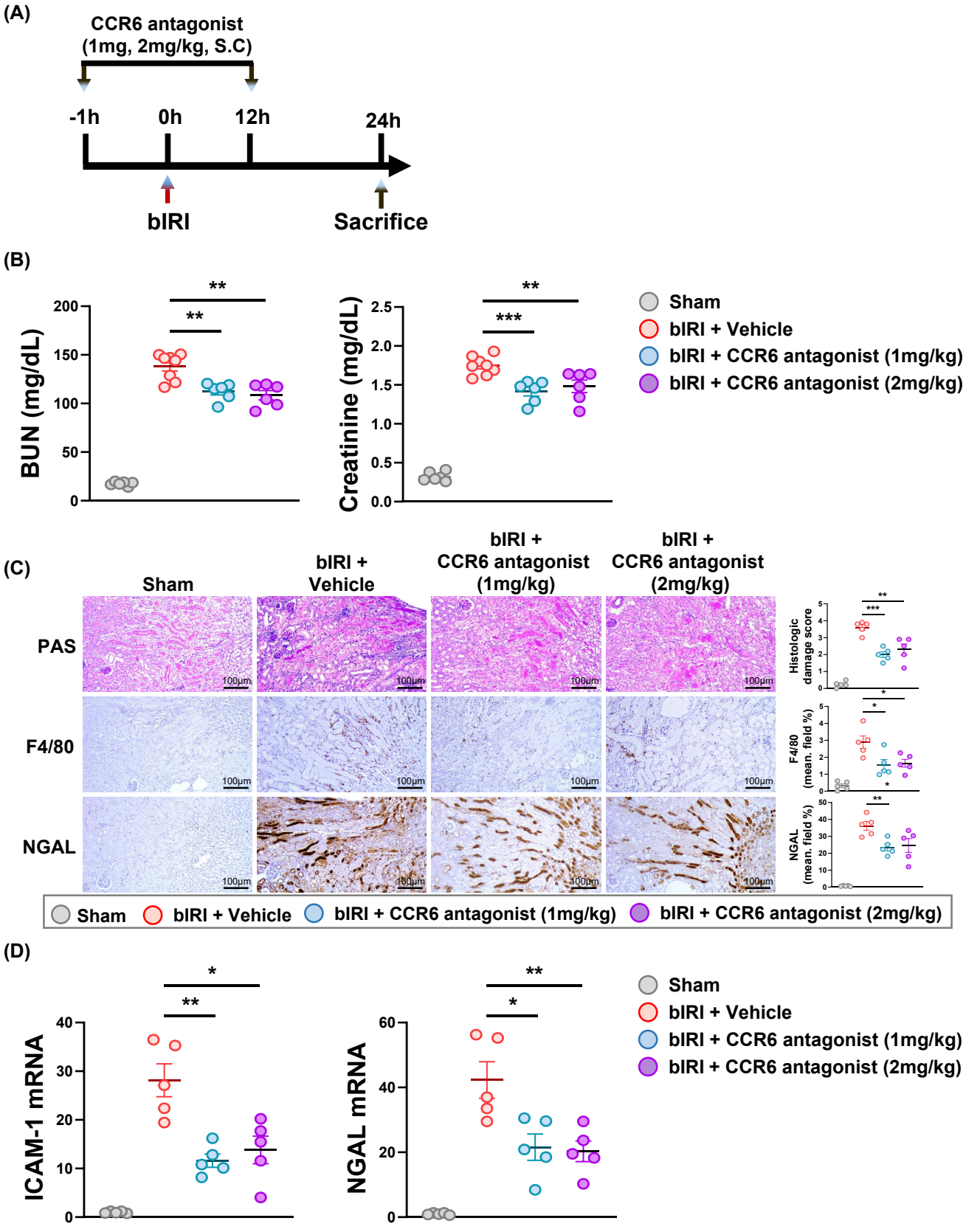

further research and experimentation are needed to comprehensively understand this intricate process. We acknowledge the need for more exhaustive studies and the development of dedicated animal models to furnish conclusive evidence for the role of the CCL20/CCR6 axis in mediating the transition from AKI to CKD.

FIGURE 7 Modulation of the CCL20/CCR6 axis mitigates AKI progression in a bilateral ischemia–reperfusion injury mouse model. To investigate the role of the CCL20/CCR6 axis in AKI progression, we employed a bilateral ischemia–reperfusion injury (IRI) mouse model (A). CCR6 antagonist was subcutaneously administered at 1 and 2 mg/kg, 1 h before and after IRI induction to assess its impact on AKI development. CCR6 antagonist treatment significantly reduced azotemia, as evidenced by marked decreases in blood urea nitrogen and creatinine levels at 24 h post-injury (B). CCR6 antagonist treatment effectively inhibited kidney damage, as indicated by decreased levels of F4/80 and NGAL in kidney tissue (C). Serum levels of ICAM-1 and NGAL mRNA substantially increased post AKI. However, CCR6 antagonist administration significantly reduced these levels, highlighting its significant impact on attenuating AKI progression (D). $*p < .05$, $**p < .01$, and $***p < .001$.

TABLE 4 Review of the literature detailing the current approaches used to study the CCL20–CCR6 axis in kidney diseases.

Study design	Model	Dose, route, and frequency	Effect	Reference
Mice	Experimental nephritis (*CCR6* mice vs. WT)	Intraperitoneal injection of 2.5 mg of nephro-toxic sheep serum per gram of mouse body weight	CCR6 KO mice showed aggravated renal injury and severity	Turner et al.[14]
Humans	Human kidney Bx IgA nephropathy ($n = 13$), MN ($n = 12$), crescentic GN ($n = 11$), and pre-implantation biopsies as controls ($n = 8$).		Increased CCR6 infiltration in tubular epithelial cells	Welsh-Bacic[18]
Humans/Mice	ANCA GN pts Anti-MPO GN model		NGAL KO mice showed aggravated renal injury and severity with increasing CCL20 levels	Schreiber[15]
Humans	IgAN patients from China		Increased CCR6 infiltration HMC stimulated by IgA1 could produce CCL20 and consequently recruit inflammatory Th17 cells to the kidneys to induce further lesions in IgA nephropathy	Lu[17]
Mice/Humans	Thy1.1 MPGN experiments IgAN patients	High-dose telmisartan versus other drug	CCR6 fold change (×4), IgAN patients	Villa[16]
Mice	Folic acid AKI		CCL20 blockade aggravated renal injury and severity	Guerrero[40]

AUTHOR CONTRIBUTIONS

Kyung Don Yoo, Mi-yeon Yu, Kyu Hong Kim, and Seung Hee Yang were involved in conducting the experiments, analyzed the results, and contributed to manuscript writing. Kyung Don Yoo, Mi-yeon Yu, Kyu Hong Kim, and Seung Hee Yang conducted the experiments to elucidate the role of CCR6 in the kidney IRI. Kyu Hong Kim and Seung Hee Yang conducted in vitro experiments to determine the functional mechanism of CCR6. Seongmin Lee, EunHee Park, Seongmin Kang, Doo-Ho Lim, Yeonhee Lee, Jeongin Song, Soie Kown, Yong Chul Kim, Dong Ki Kim, Jong Soo Lee, Yon Su Kim, and Seung Hee Yang conceived the idea for the project; Kyung Don Yoo, Mi-yeon Yu, and Seung Hee Yang assisted with revising the figures and manuscript.

ACKNOWLEDGMENTS

This work was supported by the Ulsan University Hospital Research Grant (UUH-2020-08) and this work was supported by the National Research Foundation of Korea (NRF) grant funded by the Korea government (MSIT) (No. NRF-2022R1F1A107612912). Preliminary results were

presented in a poster at the American Society of Nephrology Kidney Week Annual Meeting in Orlando, FL, 2022. The biospecimens and data used in this study were provided by the Biobank of Seoul National University Hospital, a member of Korea Biobank Network (KBN4_A03).

DISCLOSURES

The authors declare that there are no conflicts of interest.

DATA AVAILABILITY STATEMENT

The data supporting the findings of this study are available from the corresponding author, SH Yang, upon reasonable request.

ORCID

Kyung Don Yoo https://orcid.org/0000-0001-6545-6517
Mi-yeon Yu https://orcid.org/0000-0001-5112-6955
Seongmin Kang https://orcid.org/0000-0001-7566-5339
Doo-Ho Lim https://orcid.org/0000-0002-8012-7364
Yeonhee Lee https://orcid.org/0000-0002-9216-420X
Jeongin Song https://orcid.org/0009-0004-2034-1109
Soie Kown https://orcid.org/0000-0002-0878-5469
Yong Chul Kim https://orcid.org/0000-0003-3215-8681
Dong Ki Kim https://orcid.org/0000-0002-5195-7852
Yon Su Kim https://orcid.org/0000-0003-3091-2388
Seung Hee Yang https://orcid.org/0000-0002-8575-6610

REFERENCES

1. Anders HJ, Vielhauer V, Schlondorff D. Chemokines and chemokine receptors are involved in the resolution or progression of renal disease. *Kidney Int*. 2003;63:401-415.
2. Chung AC, Lan HY. Chemokines in renal injury. *J Am Soc Nephrol*. 2011;22:802-809.
3. Baba M, Imai T, Nishimura M, et al. Identification of CCR6, the specific receptor for a novel lymphocyte-directed CC chemokine LARC. *J Biol Chem*. 1997;272:14893-14898.
4. Hirota K, Yoshitomi H, Hashimoto M, et al. Preferential recruitment of CCR6-expressing Th17 cells to inflamed joints via CCL20 in rheumatoid arthritis and its animal model. *J Exp Med*. 2007;204:2803-2812.
5. Ito T, Carson WF t, Cavassani KA, Connett JM, Kunkel SL. CCR6 as a mediator of immunity in the lung and gut. *Exp Cell Res*. 2011;317:613-619.
6. Hammerich L, Bangen JM, Govaere O, et al. Chemokine receptor CCR6-dependent accumulation of γδ T cells in injured liver restricts hepatic inflammation and fibrosis. *Hepatology*. 2014;59:630-642.
7. Ransohoff RM, Trettel F. Editorial research topic "chemokines and chemokine receptors in brain homeostasis". *Front Cell Neurosci*. 2015;9:132.
8. Schutyser E, Struyf S, Van Damme J. The CC chemokine CCL20 and its receptor CCR6. *Cytokine Growth Factor Rev*. 2003;14:409-426.
9. Ranasinghe R, Eri R. Pleiotropic immune functions of chemokine receptor 6 in health and disease. *Medicines (Basel)*. 2018;5:69.
10. Kageyama Y, Ichikawa T, Nagafusa T, Torikai E, Shimazu M, Nagano A. Etanercept reduces the serum levels of interleukin-23 and macrophage inflammatory protein-3 alpha in patients with rheumatoid arthritis. *Rheumatol Int*. 2007;28:137-143.
11. Ruth JH, Shahrara S, Park CC, et al. Role of macrophage inflammatory protein-3alpha and its ligand CCR6 in rheumatoid arthritis. *Lab Invest*. 2003;83:579-588.
12. Kawashiri SY, Kawakami A, Iwamoto N, et al. Proinflammatory cytokines synergistically enhance the production of chemokine ligand 20 (CCL20) from rheumatoid fibroblast-like synovial cells in vitro and serum CCL20 is reduced in vivo by biologic disease-modifying antirheumatic drugs. *J Rheumatol*. 2009;36:2397-2402.
13. Alikhan MA, Huynh M, Kitching AR, Ooi JD. Regulatory T cells in renal disease. *Clin Transl Immunol*. 2018;7:e1004.
14. Turner JE, Paust HJ, Steinmetz OM, et al. CCR6 recruits regulatory T cells and Th17 cells to the kidney in glomerulonephritis. *J Am Soc Nephrol*. 2010;21:974-985.
15. Schreiber A, Rousselle A, Klocke J, et al. Neutrophil gelatinase-associated Lipocalin protects from ANCA-induced GN by inhibiting TH17 immunity. *J Am Soc Nephrol*. 2020;31:1569-1584.
16. Villa L, Boor P, Konieczny A, et al. Late angiotensin II receptor blockade in progressive rat mesangioproliferative glomerulonephritis: new insights into mechanisms. *J Pathol*. 2013;229:672-684.
17. Lu G, Zhang X, Shen L, et al. CCL20 secreted from IgA1-stimulated human mesangial cells recruits inflammatory Th17 cells in IgA nephropathy. *PLoS ONE*. 2017;12:e0178352.
18. Welsh-Bacic D, Lindenmeyer M, Cohen CD, et al. Expression of the chemokine receptor CCR6 in human renal inflammation. *Nephrol Dial Transplant*. 2010;26:1211-1220.
19. Yang SH, Lee JP, Jang HR, et al. Sulfatide-reactive natural killer T cells abrogate ischemia-reperfusion injury. *J Am Soc Nephrol*. 2011;22:1305-1314.
20. Lee JP, Yang SH, Lee HY, et al. Soluble epoxide hydrolase activity determines the severity of ischemia-reperfusion injury in kidney. *PLoS ONE*. 2012;7:e37075.
21. An JN, Yang SH, Kim YC, et al. Periostin induces kidney fibrosis after acute kidney injury via the p38 MAPK pathway. *Am J Physiol Renal Physiol*. 2019;316:F426-F437.
22. Lee JW, Bae E, Kwon SH, et al. Transcriptional modulation of the T helper 17/interleukin 17 axis ameliorates renal ischemia-reperfusion injury. *Nephrol Dial, Transplant*. 2019;34:1481-1498.
23. Yoo KD, Cha RH, Lee S, et al. Chemokine receptor 5 blockade modulates macrophage trafficking in renal ischaemic-reperfusion injury. *J Cell Mol Med*. 2020;24:5515-5527.
24. Park JY, Yoo KD. Blockade of STAT3 signaling alleviates the progression of acute kidney injury to chronic kidney disease through antiapoptosis. *Am J Physiol Renal Physiol*. 2022;322:F553-F572.
25. An JN, Li L, Lee J, et al. cMet agonistic antibody attenuates apoptosis in ischaemia-reperfusion-induced kidney injury. *J Cell Mol Med*. 2020;24:5640-5651.
26. Mark DO, Linden J, Macdonald T, Huang L. Selective A2A adenosine receptor activation reduces ischemia-reperfusion injury in rat kidney. *Am J Physiol Renal Physiol*. 1999;277:F404-F412.
27. Martina MG, Giorgio C, Allodi M, et al. Discovery of small-molecules targeting the CCL20/CCR6 axis as first-in-class inhibitors for inflammatory bowel diseases. *Eur J Med Chem*. 2022;243:114703.

28. Kim JE, Han D, Jeong JS, et al. Multisample mass spectrometry-based approach for discovering injury markers in chronic kidney disease. *Mol Cell Proteom*. 2021;20:100037.
29. Jo HA, Seo JH, Lee S, et al. Metabolomic profiling in kidney cells treated with a sodium glucose-cotransporter 2 inhibitor. *Sci Rep*. 2023;13:2026.
30. Kim YC, Lee J, An JN, et al. Renoprotective effects of a novel cMet agonistic antibody on kidney fibrosis. *Sci Rep*. 2019;9:13495.
31. Zhou TB, Xu HL, Qin YH, Lei FY, Huang WF, Drummen GP. LIM homeobox transcription factor 1B is associated with pro-fibrotic components and apoptosis in hypoxia/reoxygenation renal tubular epithelial cells. *Apoptosis*. 2014;19:594-602.
32. Yu J, Wu H, Liu ZY, Zhu Q, Shan C, Zhang KQ. Advanced glycation end products induce the apoptosis of and inflammation in mouse podocytes through CXCL9-mediated JAK2/STAT3 pathway activation. *Int J Mol Med*. 2017;40:1185-1193.
33. Jang HR, Gandolfo MT, Ko GJ, Satpute S, Racusen L, Rabb H. Early exposure to germs modifies kidney damage and inflammation after experimental ischemia-reperfusion injury. *Am J Physiol Renal Physiol*. 2009;297:F1457-F1465.
34. Lee SM, Yang S, Cha R-h, et al. Circulating TNF receptors are significant prognostic biomarkers for idiopathic membranous nephropathy. *PLoS ONE*. 2014;9:e104354.
35. Sharfuddin AA, Molitoris BA. Pathophysiology of ischemic acute kidney injury. *Nat Rev Nephrol*. 2011;7:189-200.
36. Funk JA, Schnellmann RG. Persistent disruption of mitochondrial homeostasis after acute kidney injury. *Am J Physiol Renal Physiol*. 2012;302:F853-F864.
37. Wang Y, Chang J, Yao B, et al. Proximal tubule-derived colony stimulating factor-1 mediates polarization of renal macrophages and dendritic cells, and recovery in acute kidney injury. *Kidney Int*. 2015;88:1274-1282.
38. Huen SC, Huynh L, Marlier A, Lee Y, Moeckel GW, Cantley LG. GM-CSF promotes macrophage alternative activation after renal ischemia/reperfusion injury. *J Am Soc Nephrol*. 2015;26:1334-1345.
39. Liu BC, Tang TT, Lv LL, Lan HY. Renal tubule injury: a driving force toward chronic kidney disease. *Kidney Int*. 2018;93:568-579.
40. Gonzalez-Guerrero C, Morgado-Pascual JL, Cannata-Ortiz P, et al. CCL20 blockade increases the severity of nephrotoxic folic acid-induced acute kidney injury. *J Pathol*. 2018;246:191-204.
41. Gaut JP, Liapis H. Acute kidney injury pathology and pathophysiology: a retrospective review. *Clin Kidney J*. 2021;14:526-536.
42. Gupta A, Puri V, Sharma R, Puri S. Folic acid induces acute renal failure (ARF) by enhancing renal prooxidant state. *Exp Toxicol Pathol*. 2012;64:225-232.
43. See EJ, Jayasinghe K, Glassford N, et al. Long-term risk of adverse outcomes after acute kidney injury: a systematic review and meta-analysis of cohort studies using consensus definitions of exposure. *Kidney Int*. 2019;95:160-172.
44. Chawla LS, Bellomo R, Bihorac A, et al. Acute kidney disease and renal recovery: consensus report of the acute disease quality Initiative (ADQI) 16 workgroup. *Nat Rev Nephrol*. 2017;13:241-257.

SUPPORTING INFORMATION

Additional supporting information can be found online in the Supporting Information section at the end of this article.

How to cite this article: Yoo KD, Yu M-y, Kim KH, et al. Role of the CCL20/CCR6 axis in tubular epithelial cell injury: Kidney-specific translational insights from acute kidney injury to chronic kidney disease. *The FASEB Journal*. 2024;38:e23407. doi:10.1096/fj.202301069RR